

High Operating Temperature HgCdTe Coupled Cavity Plasmonic Infrared Photodetectors: supplemental document

In the Supplement 1 we report in Section 1 details about the derivation of the Hamiltonian and the method followed for its diagonalization, and in Section 2 the HgCdTe parameters and material models employed throughout the present work.

1. DERIVATION OF THE HAMILTONIAN

The Hamiltonian describing the SPP-OC interacting system includes three terms (we neglect any interaction with external environment, reservoir, etc.):

$$\hat{H} = \hat{H}_{\text{OC}} + \hat{H}_{\text{SPP}} + \hat{H}_{\text{int}}. \quad (\text{S1})$$

Here, \hat{H}_{OC} is the free electromagnetic field Hamiltonian, whose derivation can be found in [1, 2]. As a short reminder, the electromagnetic vector potential \mathbf{A} is decomposed in normal modes,

$$\mathbf{A} = \left(\frac{\hbar}{2V\epsilon_0} \right)^{1/2} \sum_{\mathbf{q}} \frac{\hat{\zeta}}{\sqrt{\omega_{\text{OC},\mathbf{q}}}} \left(a_{\mathbf{q}}^* e^{i\mathbf{q}\mathbf{r}} + a_{\mathbf{q}} e^{-i\mathbf{q}\mathbf{r}} \right), \quad (\text{S2})$$

where $\hat{\zeta}$ is the electric field polarization unit vector, $q = (\omega/c, \mathbf{q})$ and $r = (ct, \mathbf{r})$, \mathbf{q} is the electric field wavevector and $a_{\mathbf{q}}$ are complex coefficients. Then, $a_{\mathbf{q}}^*$ and $a_{\mathbf{q}}$ are replaced by creation (destruction) operators $\hat{a}_{\mathbf{q}}^\dagger$ ($\hat{a}_{\mathbf{q}}$), which obey bosonic commutation rules, in analogy with the harmonic oscillator. From the electric and magnetic fields in the Coulomb gauge, $\mathbf{E} = -\partial\mathbf{A}/\partial t$ and $\mathbf{B} = \nabla \times \mathbf{A}$, respectively, the free OC Hamiltonian takes the standard form

$$\hat{H}_{\text{OC}} = \sum_{\mathbf{q}} E_{\text{OC},\mathbf{q}} \left(\hat{a}_{\mathbf{q}}^\dagger \hat{a}_{\mathbf{q}} + \frac{1}{2} \right), \quad (\text{S3})$$

where $E_{\text{OC},\mathbf{q}} = \hbar\omega_{\text{OC},\mathbf{q}}$ is the energy of an OC mode with wavevector \mathbf{q} .

\hat{H}_{SPP} is the Hamiltonian of the free electron plasma, whose oscillations result from the linear response to the solicitation of the harmonic electric field of the SPP propagating mode. Classically, the resulting average dipole moment of the charge distribution over some volume V can be described by a vector field \mathbf{P} with a dipole moment unit vector \hat{d} , which, in this simple formulation, lies in the same direction of $\hat{\zeta}$ (*i.e.*, along \hat{x}). We can consider a mode expansion of \mathbf{P} similar to Eq. (S2). Then, the quantization of \mathbf{P} and the subsequent derivation of \hat{H}_{SPP} proceeds as for a harmonic oscillator. The obtained expression is [3–5]

$$\hat{H}_{\text{SPP}} = \sum_{\mathbf{p}} E_{\text{SPP},\mathbf{p}} \left(\hat{b}_{\mathbf{p}}^\dagger \hat{b}_{\mathbf{p}} + \frac{1}{2} \right), \quad (\text{S4})$$

where $E_{\text{SPP},\mathbf{p}} = \hbar\omega_{\text{SPP},\mathbf{p}}$ is the energy of a SPP mode with wavevector \mathbf{p} , and $\hat{b}_{\mathbf{p}}^\dagger$ ($\hat{b}_{\mathbf{p}}$) are the bosonic operators for the creation (destruction) of plasmons.

A. SPP-OC interaction Hamiltonian

The interaction Hamiltonian can be derived within the principle of minimal coupling [6] and written in the electrical dipole gauge as [5, 7, Ch. 4]

$$H_{\text{int}} = \int d^3\mathbf{r} \frac{1}{\epsilon_0\epsilon_r(\mathbf{r})} \left[-\mathbf{D}(\mathbf{r}) \cdot \mathbf{P}(\mathbf{r}) + \frac{1}{2} \mathbf{P}^2(\mathbf{r}) \right], \quad (\text{S5})$$

and it is valid for non-magnetic materials. Here, $\mathbf{D}(\mathbf{r}) = -\epsilon(\mathbf{r})\partial\mathbf{A}(\mathbf{r})/\partial t$ is the electrical displacement field, $\epsilon = \epsilon_0\epsilon_r$ is the dielectric permittivity, ϵ_0 and ϵ_r are the vacuum and relative

permittivity, respectively. The quadratic interaction term \mathbf{P}^2 describes the self-interaction of the polarization modes, and therefore contains the effects of the dipole-dipole plasmonic interactions.

After elevating all the fields to the role of operators, $\hat{\mathbf{D}}$ can be expressed from the time-evolution of $\hat{\mathbf{A}}$ according to the Heisenberg equation,

$$\begin{aligned}\hat{\mathbf{D}} &= -\epsilon_0\epsilon_r \frac{d\hat{\mathbf{A}}}{dt} = \epsilon_0\epsilon_r \frac{i}{\hbar} [\hat{\mathbf{A}}, \hat{H}_{\text{OC}}] = \epsilon_0\epsilon_r \frac{i}{\hbar} \sum_{\mathbf{j}} \hbar\omega_{\text{OC},\mathbf{j}} [\hat{\mathbf{A}}, \hat{a}_{\mathbf{j}}^\dagger \hat{a}_{\mathbf{j}}] \\ &= -i\epsilon_r \left(\frac{\epsilon_0\hbar}{2V} \right)^{1/2} \sum_{\mathbf{q}} \xi \sqrt{\omega_{\text{OC},\mathbf{q}}} \left(\hat{a}_{\mathbf{q}}^\dagger e^{i\mathbf{q}\cdot\mathbf{r}} - \hat{a}_{\mathbf{q}} e^{-i\mathbf{q}\cdot\mathbf{r}} \right),\end{aligned}\quad (\text{S6})$$

which is consistent with [5].

Regarding $\hat{\mathbf{P}}$, it can be shown that the plasmons creation \hat{b}^\dagger and destruction \hat{b} operators must be rescaled by the square root of the carrier density N [3–5], hence they can be redefined as proportional to the plasma frequency

$$\Omega_{\text{pl}} = \left(\frac{Ne^2}{\epsilon_0\epsilon_r m^*} \right)^{1/2}, \quad (\text{S7})$$

where m^* is the electron effective mass. A good decomposition of $\hat{\mathbf{P}}$ in normal modes, which includes this constraint and has correct dimensions, is

$$\hat{\mathbf{P}} = \left(\frac{\epsilon_0\hbar}{2V} \right)^{1/2} \Omega_{\text{pl}} \sum_{\mathbf{p}} \frac{\hat{d}}{\sqrt{\omega_{\text{SPP},\mathbf{p}}}} \left(\hat{b}_{\mathbf{p}}^\dagger e^{i\mathbf{p}\cdot\mathbf{r}} + \hat{b}_{\mathbf{p}} e^{-i\mathbf{p}\cdot\mathbf{r}} \right). \quad (\text{S8})$$

The interaction Hamiltonian follows as:

$$\begin{aligned}\hat{H}_{\text{int}} &= -i \int d^3\mathbf{r} \frac{\hbar\Omega_{\text{pl}}}{2V} \sum_{\mathbf{p},\mathbf{q}} \sqrt{\frac{\omega_{\text{OC},\mathbf{q}}}{\omega_{\text{SPP},\mathbf{p}}}} \left(\hat{a}_{\mathbf{q}}^\dagger e^{i\mathbf{q}\cdot\mathbf{r}} - \hat{a}_{\mathbf{q}} e^{-i\mathbf{q}\cdot\mathbf{r}} \right) \left(\hat{b}_{\mathbf{p}}^\dagger e^{i\mathbf{p}\cdot\mathbf{r}} + \hat{b}_{\mathbf{p}} e^{-i\mathbf{p}\cdot\mathbf{r}} \right) \\ &\quad + \frac{\hbar\Omega_{\text{pl}}^2}{4\epsilon_r V} \int d^3\mathbf{r} \sum_{\mathbf{p},\mathbf{q}} \frac{1}{\sqrt{\omega_{\text{SPP},\mathbf{p}}}\omega_{\text{SPP},\mathbf{q}}} \left(\hat{b}_{\mathbf{p}}^\dagger e^{i\mathbf{p}\cdot\mathbf{r}} + \hat{b}_{\mathbf{p}} e^{-i\mathbf{p}\cdot\mathbf{r}} \right) \left(\hat{b}_{\mathbf{q}}^\dagger e^{i\mathbf{q}\cdot\mathbf{r}} + \hat{b}_{\mathbf{q}} e^{-i\mathbf{q}\cdot\mathbf{r}} \right).\end{aligned}\quad (\text{S9})$$

The spatial integration and the summation over \mathbf{q} yield

$$\hat{H}_{\text{int}} = iI_0 \frac{\hbar\Omega_{\text{pl}}}{2} \sum_{\mathbf{p}} \sqrt{\frac{\omega_{\text{OC},\mathbf{p}}}{\omega_{\text{SPP},\mathbf{p}}}} \left(\hat{a}_{\mathbf{p}}^\dagger - \hat{a}_{\mathbf{p}} \right) \left(\hat{b}_{\mathbf{p}}^\dagger + \hat{b}_{\mathbf{p}} \right) + \sum_{\mathbf{p}} \frac{\hbar\Omega_{\text{pl}}^2}{4\epsilon_r\omega_{\text{SPP},\mathbf{p}}} \left(\hat{b}_{\mathbf{p}}^\dagger + \hat{b}_{\mathbf{p}} \right)^2, \quad (\text{S10})$$

where I_0 is the overlap integral between the interacting SPP and OC modes. Moreover, if only one SPP and one OC modes are considered, the summations in Eq. (S10) accounts for just one term, leading to the simpler form

$$\hat{H}_{\text{int}} = i\gamma \left(\hat{a}^\dagger - \hat{a} \right) \left(\hat{b}^\dagger + \hat{b} \right) + \delta \left(\hat{b}^\dagger + \hat{b} \right)^2 \quad (\text{S11})$$

with SPP-OC interaction energy

$$\gamma = I_0 \frac{\hbar\Omega_{\text{pl}}}{2} \sqrt{\frac{E_{\text{OC}}}{E_{\text{SPP}}}} \quad (\text{S12})$$

and SPP-SPP dipole-dipole interaction energy

$$\delta = K_0 \frac{\left(\hbar\Omega_{\text{pl}} \right)^2}{E_{\text{SPP}}}, \quad (\text{S13})$$

coherent with [8], where K_0 is a plasmon-plasmon coupling constant. The term proportional to δ should be retained in the strong coupling regime [8, 9], but when the optical power flux is low (as for the IR detectors employed in astronomical imaging or surveillance optical systems) and the SPP-OC coupling is weak (*i.e.*, when $\gamma \ll E_{\text{OC}}$, as it happens for $t_{\text{abs}} \approx 0.8 \mu\text{m}$ in the considered detector), it can be safely discarded (however, this is a controversial point, and for a general discussion see, *e.g.*, [5, 8, 10–12]).

B. Diagonalization of the Hamiltonian

The full Hamiltonian in Eq. (S11) is similar to the one proposed by Hopfield [13, 14] and can be diagonalized by a standard procedure. By defining a vector $\hat{\vartheta} = (\hat{a} \hat{b} \hat{a}^\dagger \hat{b}^\dagger)$, \hat{H} can be written as $\hat{H} = \hat{\vartheta}^\dagger M \hat{\vartheta}$, where

$$M = \begin{pmatrix} E_{\text{OC}} & i\gamma & 0 & i\gamma \\ -i\gamma & (E_{\text{SPP}} + \delta) & i\gamma & \delta \\ 0 & -i\gamma & E_{\text{OC}} & -i\gamma \\ -i\gamma & \delta & i\gamma & (E_{\text{SPP}} + \delta) \end{pmatrix} \quad (\text{S14})$$

can be read from \hat{H} . The secular equation

$$\det(JM - EI) = 0, \quad (\text{S15})$$

where $J = \text{diag}(1, 1, -1, -1)$ and I is the identity matrix, can be solved for E , yielding the eigenvalues E_\pm

$$E_\pm^2 = \frac{E_{\text{OC}}^2 + E_{\text{SPP}}^2 + 2E_{\text{SPP}}\delta}{2} \pm \frac{1}{2} \sqrt{[E_{\text{OC}}^2 - (E_{\text{SPP}}^2 + 2E_{\text{SPP}}\delta)]^2 + 16\gamma^2 E_{\text{SPP}} E_{\text{OC}}}. \quad (\text{S16})$$

The mode splitting at the SPP-OC crossing is defined as

$$\Delta = (E_+ - E_-)|_{E_{\text{SPP}}=E_{\text{OC}}} \approx 2\gamma \quad (\text{S17})$$

where the last approximated equality holds only if $\gamma \ll E_{\text{OC}}$. We can accept it as a rough estimate and express Δ as

$$\Delta = 2\gamma = I_0 \hbar \Omega_{\text{pl}}, \quad (\text{S18})$$

which implies $E_+ \approx E_{\text{OC}} + \Delta/2$ and $E_- \approx E_{\text{OC}} - \Delta/2$, not a rigorously valid result in the general case of strong coupling.

As we observed in the text, an alternative approach could be to remain within the classical electrodynamics. By following the coupled mode theory, an expression simplified with respect to Eq. (S16) can be found [15],

$$E_\pm = \frac{E_{\text{OC}} + E_{\text{SPP}}}{2} \pm \frac{1}{2} \sqrt{(E_{\text{OC}} - E_{\text{SPP}})^2 + 4\gamma^2}. \quad (\text{S19})$$

It can be observed that in this expression enter the energies instead of their squares as it happens in Eq. (S16). Moreover, it is important to remark that Eq. (S19) can be obtained also within our quantum mechanical formalism, by reducing it to the rotating wave approximation (RWA). The latter is obtained by neglecting the term in \mathbf{P}^2 in the interaction Hamiltonian – hence, setting $\delta = 0$ in Eq. (S11)) and also the counter-rotating terms proportional to the products $\hat{a}^\dagger \hat{b}^\dagger$ and $\hat{a} \hat{b}$ in the same Eq. (S11). We emphasize that the RWA or the coupled-mode theory do not correctly describe the strong-coupling scenarios [5, 8], nevertheless they enlighten what is, in this context, the classical limit of the full quantum description.

The FDTD simulations presented in this article are based on the solutions of Maxwell's equations. Strictly speaking, therefore, the location of high absorption stripes in the presented color maps of the responsivity should be compared with the Hamiltonian eigenvalues provided by the Eq. (S19). Nevertheless, the differences between the values for E_\pm provided by this equation (RWA description) and the Eq. (S16) (quantum mechanical description) are quite small for the investigated detectors anyway, as can be seen in Fig. S1, and both descriptions can be employed. Conversely, in the strong-coupling regime, *i.e.*, if $\gamma/E_{\text{OC}} \approx 1$, the description provided by the RWA would be unacceptable. In general, especially with regard to possible investigations and comparison with experimental data, however, the Eq. (S16) should always be used.

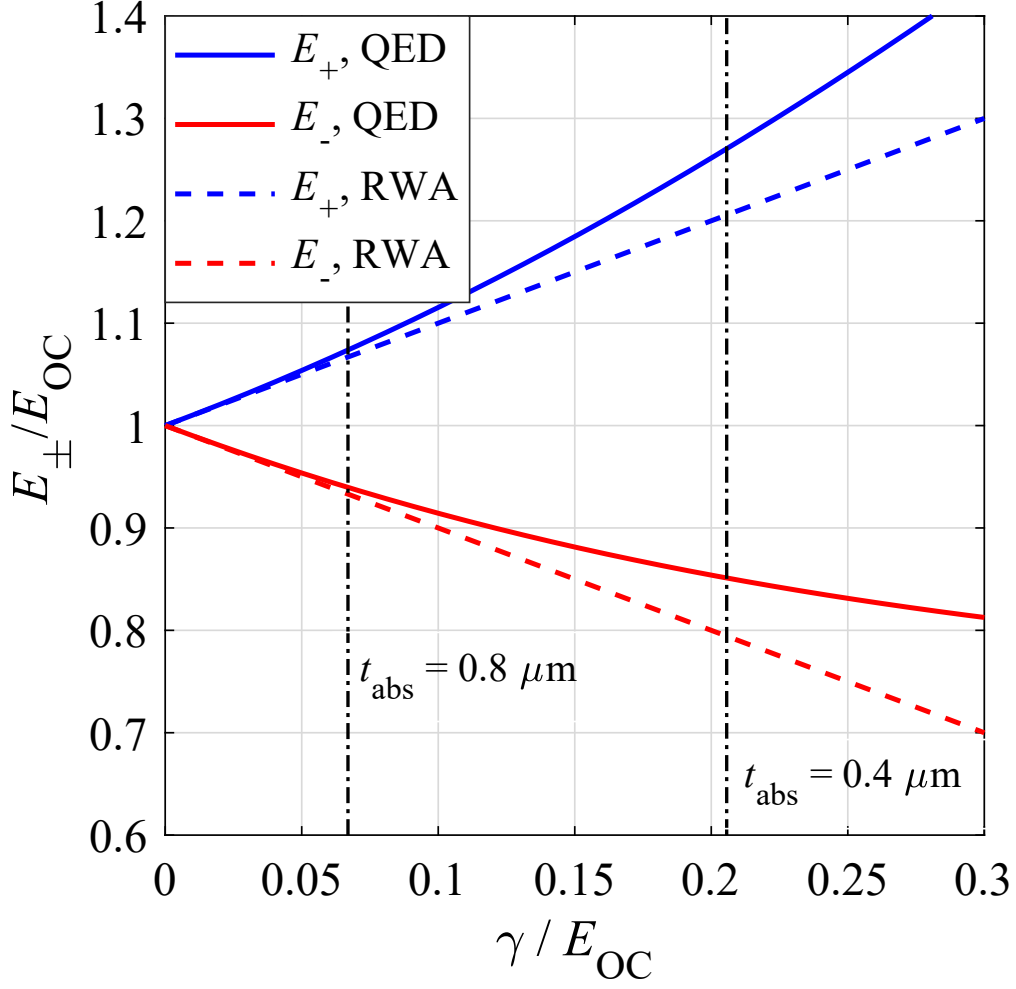


Fig. S1. Eigenvalues E_{\pm} at the crossing $E_{OC} = E_{SPP}$, calculated within the described full quantum electrodynamics formalism (QED, Eq. (S16), with $K_0 = 1$) and within classical electrodynamics, or rotating-wave approximation (RWA, Eq. (S19)). The values of γ/E_{OC} corresponding to $t_{\text{abs}} = 0.4 \mu\text{m}$ and $t_{\text{abs}} = 0.8 \mu\text{m}$, according to Eq. (S17), are marked as vertical lines. In the worst case ($t_{\text{abs}} = 0.4 \mu\text{m}$), the difference is a blue-shift around 6%.

2. MATERIAL PARAMETERS

Table S1. Material parameters for $\text{Hg}_{1-x}\text{Cd}_x\text{Te}$ used in the present simulations.

Parameter	References
$E_g(x, T) = -0.302 + 1.93x - 0.81x^2 + 0.832x^3 + 5.35 \times 10^{-4} \left(\frac{T^3 - 1822}{T^2 + 255.2} \right) (1 - 2x)$	[16, p. 1243]
$\chi(x, T) = 4.23 - 0.813 (E_g(x, T) - 0.083)$	[17, p. 1331]
$m_e(x, T) = \frac{m_0}{1 + 2F + \frac{1}{3}E_p \left(\frac{2}{E_g(x, T)} + \frac{1}{E_g(x, T) + \delta} \right)}$, where $E_p = 19 \text{ eV}$, $\delta = 1 \text{ eV}$, $F = -0.8$ $m_h = 0.55 m_0$	[18]
$\mu_e(x, T) = 9 \times 10^8 \left(\frac{0.2}{x} \right)^{7.5} \frac{1}{Z^{2(\frac{0.2}{x})^{0.6}}}$, where $Z = \begin{cases} T & \text{if } T > 50 \text{ K} \\ \frac{1.18 \times 10^5}{2600 - T - 35 ^{2.07}} & \text{if } T \leq 50 \text{ K} \end{cases}$ $\mu_h(x, T) = \frac{\mu_e(x, T)}{100}$	[19, Eq. 14.7]
$B = \hat{B} \epsilon_\infty^{1/2} \left(\frac{1}{m_e(x) + m_h} \right)^{3/2} \left(1 + \frac{1}{m_e(x)} + \frac{1}{m_h} \right) \left(\frac{300}{T} \right)^{3/2} (E_g(x, T)^2 + 3k_B T E_g(x, T) + 3.75(k_B T)^2)$ $\hat{B} = 5.8 \times 10^{-13} \text{ cm}^{-3} \text{ s}^{-1}$	[20, Eqs. 5, 9]
$C_n(x, T) = \frac{1}{2n_i^2 \tau_{A1}^i}$, $C_p(x, T) = \frac{C_n(x, T)}{\gamma} \left(\frac{1 - \frac{3E_g(x, T)}{2k_B T}}{1 - \frac{5E_g(x, T)}{4k_B T}} \right)$, where $\gamma = 6$, $\tau_{A1}^i(x, T) = \hat{\tau} \epsilon_\infty^2 \sqrt{1 + \frac{m_e(x, T)}{m_h}} \left(1 + 2 \frac{m_e(x, T)}{m_h} \right) \frac{\exp(A_0(x, T))}{B_0(x, T)}$, $\hat{\tau} = 3.8 \times 10^{-18} \text{ s}$ $A_0(x, T) = \left(\frac{1 + 2 \frac{m_e(x, T)}{m_h}}{\frac{m_e(x, T)}{1 + \frac{m_e(x, T)}{m_h}}} \right) \frac{E_g(x, T)}{k_B T}$, $B_0(x, T) = m_e(x, T) F_{12} ^2 \left(\frac{k_B T}{E_g(x, T)} \right)^{1.5}$, $F_{12} = 0.2$	[20–22, Eqs. 5, 9]
$\epsilon_0(x) = 20.5 - 15.5x + 5.7x^2$, $\epsilon_\infty(x) = 15.2 - 13.7x + 6.4x^2$	[17]
$n_i(x, T) = \tilde{n}_i n_{i0}(x, T) E_g(x, T)^{\frac{3}{4}} T^{3/2} \exp\left(-\frac{E_g(x, T)}{2k_B T}\right)$, where $\tilde{n}_i = 10^{14} \text{ cm}^{-3}$ $n_{i0}(x, T) = 5.24256 - 3.5729x - 4.74019 \times 10^{-4}T + 1.25942 \times 10^{-2}xT - 5.77046x^2 - 4.24123 \times 10^{-6}T^2$	[23]
$\alpha(x) = \begin{cases} \alpha_0(x) \exp\left(\frac{\sigma(x)(h\nu - E_0(x))}{T + T_0}\right) & \text{if } h\nu < E_T(x) \\ \alpha_T(x) \sqrt{\frac{2\sigma(x)}{T + T_0}} \left[h\nu - \left(E_T(x) - \frac{T + T_0}{2\sigma(x)} \right) \right] & \text{if } h\nu \geq E_T(x) \end{cases}$ $\alpha_0(x) = \exp(-18.88 + 53.61x)$ $\alpha_T(x) = 100 + 5000x$, $T_0 = 81.9 \text{ K}$, $\sigma(x) = 3.267 \times 10^4 (1 + x)$, $E_0(x) = 1.838x - 0.3424 \text{ eV}$, $E_T(x) = E_0(x) + \frac{T + T_0}{\sigma(x)} \ln\left(\frac{\alpha_T(x)}{\alpha_0(x)}\right)$	[24]

REFERENCES

1. M. E. Peskin and D. V. Schroeder, *Quantum Field Theory* (CRC Press, Boca Raton (FL), US, 1995).
2. F. Mandl and B. Shaw, *Quantum Field Theory, 2nd Edition* (Wiley, UK, 2010).
3. C. Ciuti, G. Bastard, and I. Carusotto, "Quantum vacuum properties of the intersubband cavity polariton field," *Phys. Rev. B* **72**, 115303 (2005).
4. S. D. Liberato and C. Ciuti, "Stimulated scattering and lasing of intersubband cavity polaritons," *Phys. Rev. Lett.* **102**, 136403 (2009).
5. Y. Todorov and C. Sirtori, "Intersubband polaritons in the electrical dipole gauge," *Phys. Rev. B* **85**, 045304 (2012).
6. J. Rammer, *Quantum Field Theory of Non-equilibrium States* (Cambridge University Press, Cambridge, U.K., 2007).
7. C. Cohen-Tannoudji, J. Dupont-Roc, and G. Grynberg, *Photons and Atoms: Introduction to Quantum Electrodynamics* (John Wiley & Sons, New York, 1997).
8. N. S. Mueller, Y. Okamura, B. G. M. Vieira, *et al.*, "Deep strong light-matter coupling in plasmonic nanoparticle crystals," *Nature* **583**, 780 (2020).
9. Z. Wang, L. Li, S. Wei, *et al.*, "Manipulating light-matter interaction into strong coupling regime for photon entanglement in plasmonic lattices," *J. Appl. Phys.* **133**, 063101 (2023).
10. A. Vasanelli, Y. Todorov, and C. Sirtori, "Ultra-strong light-matter coupling and superradiance using dense electron gases," *C. R. Phys.* **17**, 861–873 (2016).
11. A. F. Kockum, A. Miranowicz, S. D. Liberato, *et al.*, "Ultrastrong coupling between light and matter," *Nat. Rev. Phys.* **1**, 19–40 (2019).
12. D. G. Baranov, B. Munkhbat, E. Zhukova, *et al.*, "Ultrastrong coupling between nanoparticle plasmons and cavity photons at ambient conditions," *Nat. Commun.* **11**, 2715 (2020).
13. R. H. Dicke, "Coherence in spontaneous radiation processes," *Phys. Rev.* **93**, 99–110 (1954).
14. J. J. Hopfield, "Theory of the contribution of excitons to the complex dielectric constant of crystals," *Phys. Rev.* **112**, 1555–1567 (1958).
15. H. A. Haus and W. Huang, "Coupled-mode theory," *Proc. IEEE* **79**, 1505–1518 (1991).
16. D. G. Seiler, J. R. Lowney, C. L. Litter, and M. R. LoLoee, "Temperature and composition dependence of the energy gap of $\text{Hg}_{1-x}\text{Cd}_x\text{Te}$ by two-photon magnetoabsorption technique," *J. Vac. Sci. Technol. A* **8**, 1237–1244 (1990).
17. J. Wenus, J. Rutkowski, and A. Rogalski, "Two-dimensional analysis of double-layer heterojunction HgCdTe photodiodes," *IEEE Trans. Electron Devices* **48**, 1326–1332 (2001).
18. M. H. Weiler, "Magneto-optical properties of $\text{Hg}_{1-x}\text{Cd}_x\text{Te}$ alloys," in *Defects, (HgCd)Se, (HgCd)Te*, vol. 16 of *Semiconductors and Semimetals* R. K. Willardson and A. C. Beer, eds. (Academic Press, New York, 1981), chap. 3, pp. 119–191.
19. A. Rogalski, *Infrared Detectors* (CRC Press, Boca Raton, FL, 2011), 2nd ed.
20. V. C. Lopes, A. J. Syllaios, and M. C. Chen, "Minority carrier lifetime in mercury cadmium telluride," *Semicond. Sci. Technol.* **8**, 824–841 (1993).
21. T. Casselman, "Calculation of the Auger lifetime in p -type $\text{Hg}_{1-x}\text{Cd}_x\text{Te}$," *J. Appl. Phys.* **52**, 848–854 (1981).
22. F. Bertazzi, M. Goano, and E. Bellotti, "Calculation of Auger lifetime in HgCdTe ," *J. Electron. Mater.* **40**, 1663–1667 (2011).
23. J. R. Lowney, D. G. Seiler, C. L. Littler, and I. T. Yoon, "Intrinsic carrier concentration of narrow-gap mercury cadmium telluride based on the nonlinear temperature dependence of the band gap," *J. Appl. Phys.* **71**, 1253–1258 (1992).
24. C. A. Hougen, "Model for infrared absorption and transmission of liquid-phase epitaxy $\text{Hg}_{1-x}\text{Cd}_x\text{Te}$," *J. Appl. Phys.* **66**, 3763–3766 (1989).